(4)

David Taylor Research Center
Bethesda, MD 20084–5000

DTRC–SME–89/111 January 1990
Ship Materials Engineering Department
Research & Development Report

Damping Capacity of Aluminum 6061–Indium Alloys

by
C.R. Wong
O. Diehm*
D.C. Van Aken*

*Department Materials Science and Engineering
University of Michigan
Ann Arbor, MI 48109

Damping Capacity of Aluminum 6061–Indium Alloys
DTRC–SME–89/111

MAJOR DTRC TECHNICAL COMPONENTS

CODE 011 DIRECTOR OF TECHNOLOGY, PLANS AND ASSESSMENT

12 SHIP SYSTEMS INTEGRATION DEPARTMENT

14 SHIP ELECTROMAGNETIC SIGNATURES DEPARTMENT

15 SHIP HYDROMECHANICS DEPARTMENT

16 AVIATION DEPARTMENT

17 SHIP STRUCTURES AND PROTECTION DEPARTMENT

18 COMPUTATION, MATHEMATICS & LOGISTICS DEPARTMENT

19 SHIP ACOUSTICS DEPARTMENT

27 PROPULSION AND AUXILIARY SYSTEMS DEPARTMENT

28 SHIP MATERIALS ENGINEERING DEPARTMENT

DTRC ISSUES THREE TYPES OF REPORTS:

1. **DTRC reports, a formal series,** contain information of permanent technical value. They carry a consecutive numerical identification regardless of their classification or the originating department.

2. **Departmental reports, a semiformal series,** contain information of a preliminary, temporary, or proprietary nature or of limited interest or significance. They carry a *departmental alphanumerical identification.*

3. **Technical memoranda, an informal series,** contain technical documentation of limited use and interest. They are primarily working papers intended for internal use. They carry an identifying number which indicates their type and the numerical code of the originating department. Any distribution outside DTRC must be approved by the head of the originating department on a case-by-case basis.

NDW-DTNSRDC 5602/51 (Rev 2-88)

REPORT DOCUMENTATION PAGE

1a. REPORT SECURITY CLASSIFICATION: Unclassified	1b. RESTRICTIVE MARKINGS
2a. SECURITY CLASSIFICATION AUTHORITY	3. DISTRIBUTION/AVAILABILITY OF REPORT: Approved for public release; distribution is unlimited.
2b. DECLASSIFICATION/DOWNGRADING SCHEDULE	
4. PERFORMING ORGANIZATION REPORT NUMBER(S): DTRC-SME-89/111	5. MONITORING ORGANIZATION REPORT NUMBER(S)
6a. NAME OF PERFORMING ORGANIZATION: David Taylor Research Center; 6b. OFFICE SYMBOL (If applicable): Code 2812	7a. NAME OF MONITORING ORGANIZATION
6c. ADDRESS (City, State, and ZIP Code): Annapolis, MD 21401	7b. ADDRESS (City, State, and ZIP Code)
8a. NAME OF FUNDING/SPONSORING ORGANIZATION: David Taylor Research Center; 8b. OFFICE SYMBOL (If applicable): Code 0115	9. PROCUREMENT INSTRUMENT IDENTIFICATION NUMBER
8c. ADDRESS (City, State, and ZIP Code): Bethesda, MD 20084-5000	10. SOURCE OF FUNDING NUMBERS: PROGRAM ELEMENT NO. 62234N; PROJECT NO.; TASK NO. RS34S94; WORK UNIT ACCESSION NO. DN507603

11. TITLE (Include Security Classification): Damping Capacity of Aluminum 6061–Indium Alloys

12. PERSONAL AUTHOR(S): C.R. Wong, O. Diehm and D.C. Van Aken

13a. TYPE OF REPORT	13b. TIME COVERED	14. DATE OF REPORT (YEAR, MONTH, DAY)	15. PAGE COUNT
Research and Development	FROM 10/87 TO 2/89	January 1990	22

16. SUPPLEMENTARY NOTATION

17. COSATI CODES			18. SUBJECT TERMS (Continue on reverse if necessary and identify by block number)
FIELD	GROUP	SUB-GROUP	Damping, Modulus, 6061–Aluminum, Complex Modulus, JET

19. ABSTRACT (Continue on reverse if necessary and identify by block number)

Monotectic Al–6061 alloys containing between 0 and 5.2 volume percent indium and pure indium samples were fabricated. Each sample was characterized by metallographic and analytical electron microscopy and the damping capacity and storage modulus were measured. The model proposed by L.G. Nielsen was used to calculate the damping capacity and storage modulus of the alloys using the damping capacity and storage modulus of the constituents. The damping capacity of the Al-6061-T6 alloy and increased with increasing indium content. The Nielsen model gave a good first approximation of the damping capacity and storage modulus of the alloys.

20. DISTRIBUTION/AVAILABILITY OF ABSTRACT	21. ABSTRACT SECURITY CLASSIFICATION
☐ UNCLASSIFIED/UNLIMITED ☒ SAME AS RPT ☐ DTIC USERS	Unclassified

22a. NAME OF RESPONSIBLE INDIVIDUAL	22b. TELEPHONE (Include Area Code)	22c. OFFICE SYMBOL
C.R. Wong	(301) 267–2835	Code 2812

CONTENTS

ABSTRACT.....1

ADMINISTRATIVE INFORMATION.....1

INTRODUCTION.....1

NIELSEN MODEL.....2

EXPERIMENTAL PROCEDURE.....7

RESULTS.....8

DISCUSSION.....10

CONCLUSIONS.....11

ACKNOWLEDGMENTS.....12

REFERENCES.....13

FIGURES

Figure 1: Single Cantilever Clamping Arrangement of the Dynamic Mechanical Thermal Analyzer.....14

Figure 2: Microstructures of 6061-T6 Aluminum with 1.4 - 5.2 Volume Percent Indium.....15

Figure 3: Precipitates in 6061-T6 Aluminum with 0 - 5.2 Volume Percent Indium.....16

Figure 4: Values of the Loss Factor and Storage Modulus of the Monolithic Materials Measured from 20 to 100°C at 0.1 Hz.....17

Figure 5: Values of the Loss Factor and Storage Modulus of 6061 Aluminum with 0 to 2.7 Volume Percent Indium Measured from 20 to 100°C at 0.1 Hz.....18

Figure 6: Values of the Loss Factor and Storage Modulus of 6061 Aluminum with 0 to 5.2 Volume Percent Indium Measured from 20 to 100°C at 0.1 Hz.....19

Figure 7: Values of the Loss Factor and Storage Modulus of 6061 Aluminum with 0 to 2.7 Volume Percent Indium Calculated Using Nielsens Model.....20

Figure 8: Comparison of Measured and Calculated Values of the Loss factor and Storage Modulus of 6061 Aluminum with 0 to 2.7 Volume Percent Indium.....21

Figure 9: Comparison of Measured and Calculated Values of the Loss Factor and Storage Modulus of 6061 Aluminum with 5.2 Volume Percent Indium.....22

TABLE

Table 1: Chemical Composition of Al-6061-In-T6 Alloys.....13

ABSTRACT

Type 6061 aluminum alloys containing between 0 and 5.2 volume percent indium and pure indium samples were fabricated. Each sample was characterized by metallographic and analytical electron microscopy and the damping capacity and storage modulus were measured. The model proposed by L. G. Nielsen was used to calculate the damping capacity and storage modulus of the alloys using the damping capacity and storage modulus of pure indium and 6061 aluminum. The damping capacity of the Al-6061-In-T6 alloys were higher than the Al-6061-T6 alloy and increased with increasing indium content. The Nielsen model gave a good first approximation of the damping capacity and storage modulus of the alloys.

ADMINISTRATIVE INFORMATION

This report was prepared under the Quiet Alloys program, part of the Functional Materials Block Program, under the sponsorship of Mr. Ivan Caplan, David Taylor Research Center (DTRC Code 0115). Work was performed at the David Taylor Research Center and the Department of Materials Science and Engineering, University of Michigan, Ann Arbor. The work was supervised by Dr. O. P. Arora, DTRC Code 2812, under Program Element 62234N, Task Area RS34S94, Work Unit 1-2812-949. This report satisfies FY89 Milestone 94SR1/6.

INTRODUCTION

An important characteristic of a structural material is it's damping capacity. While metallic materials exhibit adequate stiffness for structural use, the damping capacity may be quite low, having a typical loss factor on the order of 10^{-4}. In contrast, polymeric materials exhibit very high damping, with loss factors on the order of one, but rather low stiffness. Their stiffness can be increased with the use of fillers and fibers but the resultant resin matrix composites exhibit lower damping properties, with loss factors on the order of 10^{-2}. Attempts made to improve the damping response of the resin matrix composite by adding rubber did not result in significant improvements [1]. It was shown that synergistic effects from interactions

between the rubber and the resin were responsible for the lower than expected damping behavior.

In the case of metal matrix composites, work by Ray, Kinra, Rawal and Misra has shown that the damping of aluminum alloy 6061 is increased by the addition of graphite fibers [2]. However, the increase in damping was low considering the high volume fraction (0.34) of graphite. Recent work by Diehm, Wong and Van Aken has shown that the addition of a viscoelastic inclusion (indium) to pure aluminum will produce high damping materials [3], but it was uncertain whether the principal damping resulted from the matrix or the inclusion since both have high damping capacities.

In this investigation the addition of indium, an elastically soft second phase particle, to 6061 T6 aluminum, a stiff matrix, was examined in order to differentiate between inclusion and matrix damping. Additionally the model to predict the stiffness of composite materials proposed by L. G. Nielsen [4,5] was evaluated for its ability to predict the damping capacity of composite materials. The dynamic properties of pure (99.99%) indium and 6061 T6 aluminum were determined. The dynamic properties of the composite were calculated using the values of the monolithic materials in the Nielsen model and directly compared with the experimental results.

NIELSEN MODEL

The model developed by Nielsen [4] predicts the complex modulus of isotropic two phase materials with arbitrary phase geometry. It is based on a continuum mechanics composite sphere assemblage model but is semi-empirical. The model assumes that the alloy is isotropic, strained only in the elastic range, and is phase symmetric, that is both the matrix and second phase geometries are identical at equal respective volume concentrations. Equations

1-4 below, from Nielsen's model [5], can be used to calculate Young's modulus of the alloy, E_y, using the Young's moduli of the matrix, E_y^s, and second phase, E_y^i, and the volume concentration, c. The volume concentration = $\frac{V^i}{(V^s + V^i)}$ where V^i and V^s are the volumes of the second phase and matrix respectively.

$$E_y = eE_y^s \qquad \text{eq.1}$$

where e is the relative Young's modulus of the alloy.

$$e = \frac{n + \gamma + \gamma c(n - 1)}{n + \gamma - c(n - 1)} \qquad \text{eq.2}$$

where n is the relative stiffness and γ is the shape function.

$$n = \frac{E_y^i}{E_y^s} \qquad \text{eq.3}$$

$$\gamma = \frac{1}{2}\left\{ \rho[1 - c(1 - n)] + \sqrt{\rho^2[1 - c(1 - n)]^2 + 4n(1 - \rho)} \right\} \qquad \text{eq.4}$$

where ρ is the shape factor which is dependent on the morphology of the composite.

The complex modulus of the matrix, E^i, and second phase, E^s, is defined as follows.

$$E^s = a^s + b^s i \text{ and } E^i = a^i + b^i \qquad \text{eq.5}$$

where a and b are the storage and loss modulus respectively and the superscripts s and i refer to the matrix and second phase respectively. The conversion from Young's modulus equations to complex modulus equations is accomplished with the use of the correspondence principle. The complex moduli from equation 5 are substituted for the Young's moduli in equations 1 and 3 and the real and imaginary parts are separated. Starting with equation 3:

$$n = \frac{E^i}{E^s} = \frac{a^i + ib^i}{a^s + ib^s} = \frac{(a^i + ib^i)(a^s - ib^s)}{(a^s + ib^s)(a^s - ib^s)} = \frac{a^ia^s + b^ib^s}{(a^s)^2 + (b^s)^2} + \frac{(a^sb^i - a^ib^s)i}{(a^s)^2 + (b^s)^2}$$

Let $n = A + Bi$ where $A = \frac{a^ia^s + b^ib^s}{(a^s)^2 + (b^s)^2}$ and $B = \frac{a^sb^i - a^ib^s}{(a^s)^2 + (b^s)^2}$ eq.6

Now recalling equation 4

$$\gamma = \frac{1}{2}\left\{ \rho[1 - c(1 - n)] + \sqrt{\rho^2[1 - c(1 - n)]^2+4n(1 - \rho)} \right\}$$

Upon substitution of equation 6 the first part of equation 4 becomes

$$\rho[1 - c(1 - n)] = \rho - \rho c + \rho cn = \rho - \rho c + \rho cA + \rho cBi \qquad \text{eq.7}$$

The second part of equation 4 is $\sqrt{\rho^2[1 - c(1 - n)]^2+4n(1 - \rho)}$

$$[1 - c(1 - n)]^2 = 1 - 2c(1 - n) + c^2(1 - n)^2$$

$$= 1 - 2c + 22n + c^2 - 2c^2n + c^2n^2$$

$$= 1 - 2c + c^2 + (2c - 2c^2)n + c^2n^2$$

since $n^2 = (A + iB)(A + iB) = A^2 - B^2 + 2ABi$

then $[1 - c(1 - n)]^2 = (1 - 2c + c^2) + (2c - 2c^2)A + c^2(A^2 - B^2)$

$$+ i[(2c - 2c^2)B + 2c^2AB]$$

therefore $\sqrt{\rho^2[1 - c(1 - n)]^2+4n(1 - \rho)}$

$$= \left\{ \rho^2[1 - 2c + c^2 + (2c - 2c^2)A + c^2(A^2 - B^2)] \right.$$

$$\left. + i\rho^2[(2c - 2c^2)B + 2c^2AB]i + 4A(1 - \rho) + 4B(1 - \rho) \right\}^{\frac{1}{2}}$$

$$= \left\{ \rho^2[1 - 2c + c^2 + 2c(1 - c)A + c^2(A^2 - B^2)] \right.$$

$$\left. + 4A(1 - \rho) + i[\rho^2 2c(1 - c)B + 2c^2AB\rho^2 + 4B(1 - \rho)] \right\}^{\frac{1}{2}}$$

Let $\sqrt{\rho^2[1 - c(1 - n)]^2+4n(1 - \rho)} = [\alpha + \beta i]^{\frac{1}{2}}$ eq.8

where $\alpha = \rho^2[(c - 1)^2 - 2c(c - 1)A + c^2(A^2 - B^2)] + 4A(1 - \rho)$ eq.9

and $\beta = \rho^2 2c(1 - c)B + 2c^2AB\rho^2 + 4B(1 - \rho)$ eq.10

In order to find the square root the coordinates are changed.

$$r = (\alpha^2 + \beta^2)^{\frac{1}{2}} \quad \text{eq.11}$$

$$\theta = \arctan\left[\sqrt{\frac{\beta}{\alpha}}\right] \quad \text{eq.12}$$

substituting equations 11 and 12 into equation 8 results in

$$\sqrt{\rho^2[1 - c(1 - n)]^2+4n(1 - \rho)} = r^{1/2}[\cos(\theta/2)+i\sin(\theta/2)] = r^{1/2}e^{i\theta/2} \quad \text{eq.13}$$

Combining equations 7 and 13 gives the complex shape function, γ^*.

$$\gamma^* = \frac{1}{2}\left\{\rho[1 - c(1 - A)] + \rho cBi + r^{1/2}e^{i\theta/2}\right\} \qquad \text{eq.14}$$

Substituting the complex values of γ^* from equation 14 and the complex values of n from equation 6 into equation 2 gives the complex relative modulus, e^*.

$$e^* = \frac{n + \gamma^* + \gamma^* c(n - 1)}{n + \gamma^* - c(n - 1)} = \frac{n + \gamma^* + cn\gamma^* - \gamma^* c}{n + \gamma^* - cn + c}$$

$$= \frac{A + Re(\gamma^*) - cRe(\gamma^*) + c[ARe(\gamma^*) - BIm(\gamma^*)]}{(A + Re(\gamma^*) - cA + c) + (B + Im(\gamma^*) - cB)}$$

$$+ \frac{i\left\{B + Im(\gamma^*) - cIm(\gamma^*) + c[AIm(\gamma^*) + BRe(\gamma^*)]\right\}}{(A + Re(\gamma^*) - cA + c) + (B + Im(\gamma^*) - cB)} \qquad \text{eq.15}$$

Let $\xi = A + Re(\gamma^*) - cRe(\gamma^*) + c[ARe(\gamma^*) - BIm(\gamma^*)]$ eq.16

and $\eta = B + Im(\gamma^*) - cIm(\gamma^*) + c[AIm(\gamma^*) + BRe(\gamma^*)]$ eq.17

and substitute into equation 15.

$$e^* = \frac{\xi + i\eta}{(A + Re(\gamma^*) - cA + c) + (B + Im(\gamma^*) - cB)i}$$

$$= \frac{(\xi + i\eta)[(A + Re(\gamma^*) - cA + c) - (B + Im(\gamma^*) - cB)]}{(A + Re(\gamma^*) - cA + c)^2 + (B + Im(\gamma^*) - cB)^2}$$

$$= \frac{\xi(A + Re(\gamma^*) - cA + c) + \eta(B + Im(\gamma^*) - cB)}{(A + Re(\gamma^*) - cA - c)^2 + (B + Im(\gamma^*) - cB)^2}$$

$$+ \frac{i\eta(A + Re(\gamma^*) - cA + c) - \xi(B + Im(\gamma^*) - cB)}{(A + Re(\gamma^*) - cA - c)^2 + (B + Im(\gamma^*) - cB)^2} \qquad \text{eq.18}$$

Finally the complex modulus of the alloy is found by combining

equations 1, 5 and 18.

$$E^i = e^*E^s = \mathrm{Re}(e^*)a^s - \mathrm{Im}(e^*) + i[\mathrm{Im}(e^*) + \mathrm{Re}(e^*)b^s]$$

$$- \frac{a^s\left\{\xi(A + \mathrm{Re}(\gamma^*) - cA + c) + \eta(B + \mathrm{Im}(\gamma^*) - cB)\right\}}{(A + \mathrm{Re}(\gamma^*) - cA - c)^2 + (B + \mathrm{Im}(\gamma^*) - cB)^2}$$

$$- \frac{b^s\left\{\eta(A + \mathrm{Re}(\gamma^*) - cA + c) - \xi(B + \mathrm{Im}(\gamma^*) - cB)\right\}}{(A + \mathrm{Re}(\gamma^*) - cA - c)^2 + (B + \mathrm{Im}(\gamma^*) - cB)^2}$$

$$+ i\left[\frac{a^s\left\{\eta(A + \mathrm{Re}(\gamma^*) - cA + c) - \xi(B + \mathrm{Im}(\gamma^*) - cB)\right\}}{(A + \mathrm{Re}(\gamma^*) - cA - c)^2 + (B + \mathrm{Im}(\gamma^*) - cB)^2}\right.$$

$$\left. + \frac{b^s\left\{\xi(A + \mathrm{Re}(\gamma^*) - cA + c) + \eta(B + \mathrm{Im}(\gamma^*) - cB)\right\}}{(A + \mathrm{Re}(\gamma^*) - cA - c)^2 + (B + \mathrm{Im}(\gamma^*) - cB)^2}\right] \qquad \text{eq.19}$$

Where the real part of equation 19 is the storage modulus of the composite and the imaginary part of equation 19 is the loss modulus.

EXPERIMENTAL PROCEDURE

Aluminum 6061 alloys with additions of 0 to 13 weight percent indium were prepared by plasma arc-melting. The starting alloys were pure indium (99.99%) and 6061 alloy. The chemical composition of the alloys were determined by wet-chemistry. The volume fraction of indium was calculated using the weight fraction and density of each alloy by assuming complete immiscibility between aluminum and indium. The arc-melted ingot was then reduced 60 to 80% in thickness, by repeatedly cold-rolling 20 to 30% and annealing, to produce a flat sample with a nominal thickness of 1.5 mm. The alloys were given a T6 temper consisting of solution treatment at 532 °C (990 °F) and aging at 193 °C (380 °F) for 7 hours. Samples of pure indium were likewise plasma arc-melted and rolled.

Each sample was characterized by metallographic and analytical electron microscopy. Electron microscopy studies were performed at the University of Michigan Electron Microbeam Analysis Laboratory. Thin foils for transmission electron microscopy were prepared by twin jet electropolishing in a solution of 20% nitric acid (by volume) and methanol.

The damping capacity and modulus of the samples were measured with a Polymer Laboratories Dynamic Mechanical Thermal Analyzer (DMTA). The DMTA uses a fixed-guided cantilevered arrangement where the left clamp holds the sample to a stationary frame while the right clamp attaches the sample to the drive shaft as illustrated in Fig. 1. A small sinusoidal mechanical stress is applied to the cantilevered sample and the resulting sinusoidal strain is measured with a noncontacting eddy current transducer. Comparison of the amplitude of the stress, σ, and strain, ϵ, signals yields the storage modulus, a, and the phase lag of strain behind the stress gives the phase angle, δ. The complex modulus, E, and loss modulus, b, are calculated using the following equation:

$$\frac{\sigma}{\epsilon} = a(1 + i\tan\delta) = E = a + ib \qquad \text{eq.20}$$

where $\tan\delta$ is the loss factor. The frequency of the vibrations was cycled between 0.1, 1 and 10 Hz while the temperature was increased one degree C per minute from 20 °C (68 °F) to 100 °C (212 °F). Each sample was measured at least twice to check measurement consistency.

RESULTS

The measured chemical composition and the calculated volume fraction of indium are presented in table 1. The volume percent varied from 0 to 5.2. The microstructures of the indium containing alloys are shown in Fig. 2. A

uniform dispersion of indium particles was found in all the samples with the individual areas of indium increasing in size and number with the increase in volume percent. The micrographs show the indium phase to be roughly spherical. Examination of the age-hardened matrix using transmission electron microscopy revealed that the age-hardening process was affected by the addition of indium. A typical 6061 T6 microstructure consists of a uniform distribution of Guinier-Preston Zones (GPZ) and β' (rod shaped Mg_2Si) precipitates in the aluminum matrix as shown in Fig. 3a. The diffraction conditions are optimized in Figs. 3a and 3b to show the β' precipitates. The aged microstructures of the alloys containing 1.4, 1.7 and 5.2 volume percent indium are shown in Figs. 3b to 3d. It is apparent that the aging kinetics have been affected by the additions of indium. The general trend is that the precipitation of β' is inhibited and the volume fraction of second phase is reduced. Only the GPZ's are observed in the 1.7 and 5.2% alloys.

The results of the DMTA testing are shown as plots of loss factor, $\tan\delta$, versus the storage modulus on logarithmic axis in order to eliminate temperature and frequency measurement error from the data. As the temperature was increased from 20 °C to 100 °C the loss factor increased and the storage modulus decreased. The measurements of pure indium and the 6061 T6 alloy are shown in Fig. 4. For the temperature range tested, the storage modulus of the 6061 T6 alloy did not vary significantly from 71 GPa while the storage modulus of the indium varied from 2 GPa at room temperature to 0.9 GPa at 100 °C. It was generally observed that the storage modulus decreased and the loss factor increased with increasing addition of indium as shown in Fig. 5. The storage modulus of the sample containing 5.2 volume percent indium exhibited a more dramatic change than alloys containing less than 3.2 volume percent indium, as illustrated in Fig. 6. The loss factor of the 5.2

volume percent indium alloy at room temperature was measured to be 0.01. This was likely due to increased continuity of the indium phase. The storage modulus and loss factor were calculated with the Nielsen Model using the data from the monolithic material in equations 19 and 20 and a shape factor of one. A shape factor of one describes perfectly spherical second phase areas completely surrounded by the matrix. The results of these calculations are presented in Fig. 7. The calculated and measured values of the 0 volume percent indium alloy are constrained to be equal. Comparing the calculated values to the measured values as in Figs. 8 and 9 it is obvious that although the calculated values show the same trends as the measured values, they consistently overestimate both the measured storage modulus and the loss factor of the alloys. For the alloys containing less than 3.2 volume percent the storage modulus is only overestimated by 2% and the loss factor is overestimated by 30%. However, in the case of the 5.2 volume percent indium alloy the storage modulus was overestimated by more than 100% while the loss factor was overestimated by 60%. These results may indicate a synergistic effect such as the partitioning of alloying elements present in the 6061 material to the indium.

DISCUSSION

High damping aluminum alloys may be obtained by the addition of a viscoelastic inclusion. In the present case a volume fraction of at least 0.05 is required to produce an alloy with a loss factor greater than 0.01. However, there is a significant loss of stiffness associated with the addition of the indium and there appears to be a synergistic effect between the matrix and the inclusion. The aged 6061-T6 microstructure shows a decreasing precipitate density with increasing indium content and the measured loss

factors are much less than the calculated values based on the damping capacities of the monolithic samples. It is tempting to speculate that these observations are related. Indeed, the solubility of magnesium in indium is greater than 30 atomic percent at the T6 aging temperature used in this experiment [6]. Thus the low volume fraction of precipitates may be related to the partitioning of magnesium to the indium inclusions. Furthermore, The indium-magnesium inclusions may have a lower damping capacity than the pure indium. If indeed the damping of the indium inclusion is a strain dependent mechanism, such as dislocation motion, the addition of solute atoms will result in a lower loss factor for a comparable cyclic strain.

The Nielsen model failed to predict the dynamic properties of indium containing 6061 T6 alloys from the pure indium and 6061 T6 alloy properties, but did provide a good first approximation. Future modeling of this system will use the dynamic properties of monolithic indium-magnesium alloys to compensate for the synergistic effects encountered and the shape factor will be varied in an attempt to compensate for inclusions which are not perfectly spherical.

CONCLUSIONS

Additions of indium, an elastically soft second phase particle, to 6061 T6 aluminum, a stiff matrix, have resulted in an increased damping capacity while still maintaining the stiffness of the matrix. The measured and calculated values agree that the damping capacity increases and the storage modulus decreases with increasing indium content. The Nielsen model is a good first approximation for both the prediction of the maximum damping capacity and stiffness of a particular alloy system and the tailoring of

alloys to obtain the damping capacity and stiffness required by a given application.

ACKNOWLEDGMENTS

The assistance of Dr. M. A. Imam and Mr. K. Robinson of the Naval Research Laboratory with the operation of the DMTA and Mr. J. Newton of the University of Missouri Dept. of Physics with the complex algebra is greatly appreciated.

REFERENCES

1. G. Rhorauer, S. V. Hoa and D. Feldman, 5th inter. Conf. composite Materials, Eds. Harrigan, Strife, and Dhingra, The Minerals, Metals & Materials Scoiety, (1986) p. 1683.

2. A. K. Ray, V. K. Kinra, S. P. Rawal, and M. S. Misra, Role of Interfaces on Material Damping, Eds. b. B. Rath and M. S. Misra, ASM International, (1985) p. 95.

3. O. Diehm, C. R. Wong, and D. C. Van Aken, "Damping Associated with Incipient Melting in Aluminum and Al-6061-T6 Alloyed with Indium.", Proceeding of Damping 89, (1989) p. JDA1.

4. L. G. Nielsen, "Elastic Properties of Two-phase Materials", Materials Science and Engineering, 52 (1982) p 39.

5. L. G. Nielsen, "Elasticity and Damping of Porous Materials and Impregnated Materials", J. Amer. Ceramic Soc., Vol. 67, No. 2, (1984) p93

6. A. A. Nayeb-Hashemi and J. B. Clark, Bull. Alloy Phase Diagrams, Bol. 6, (1985) p.2

Table 1: Chemical Composition of Al-6061-In-T6 Alloys

Calculated Volume Percent Indium	Measured Weight Percent Indium	Magnesium	Chromium	Silicon	Copper	Iron	Aluminum
0.00	0.00	0.77	0.048	0.71	0.26	0.23	98.97
0.78	2.08	0.74	0.047	0.83	0.27	0.25	95.78
1.43	3.77	0.70	0.046	0.76	0.26	0.24	94.22
1.67	4.37	0.67	0.045	0.73	0.25	0.22	93.72
2.16	5.63	0.70	0.044	0.75	0.26	0.22	92.40
2.66	6.87	0.73	0.045	0.71	0.25	0.21	91.19
3.20	8.20	0.73	0.041	0.70	0.28	0.22	89.83
5.16	12.80	0.70	0.042	0.64	0.23	0.20	85.39

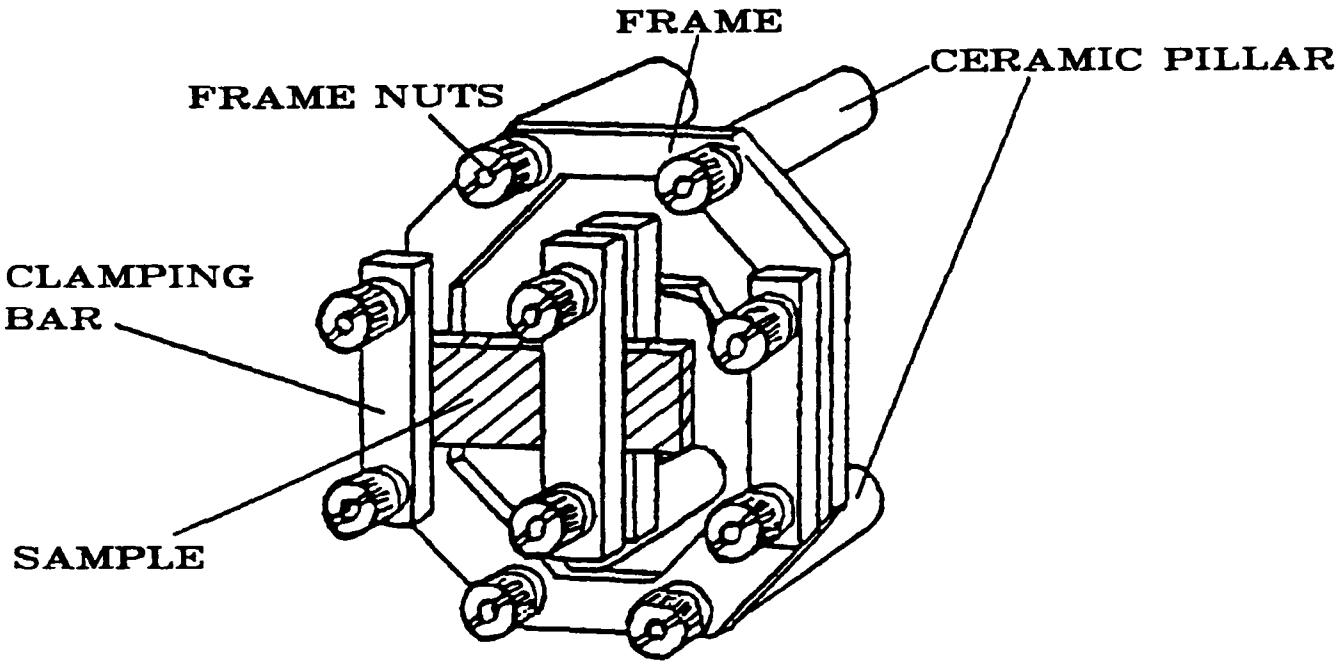

Fig. 1. Single cantilever clamping arrangement of the dynamic mechanical thermal analyzer.

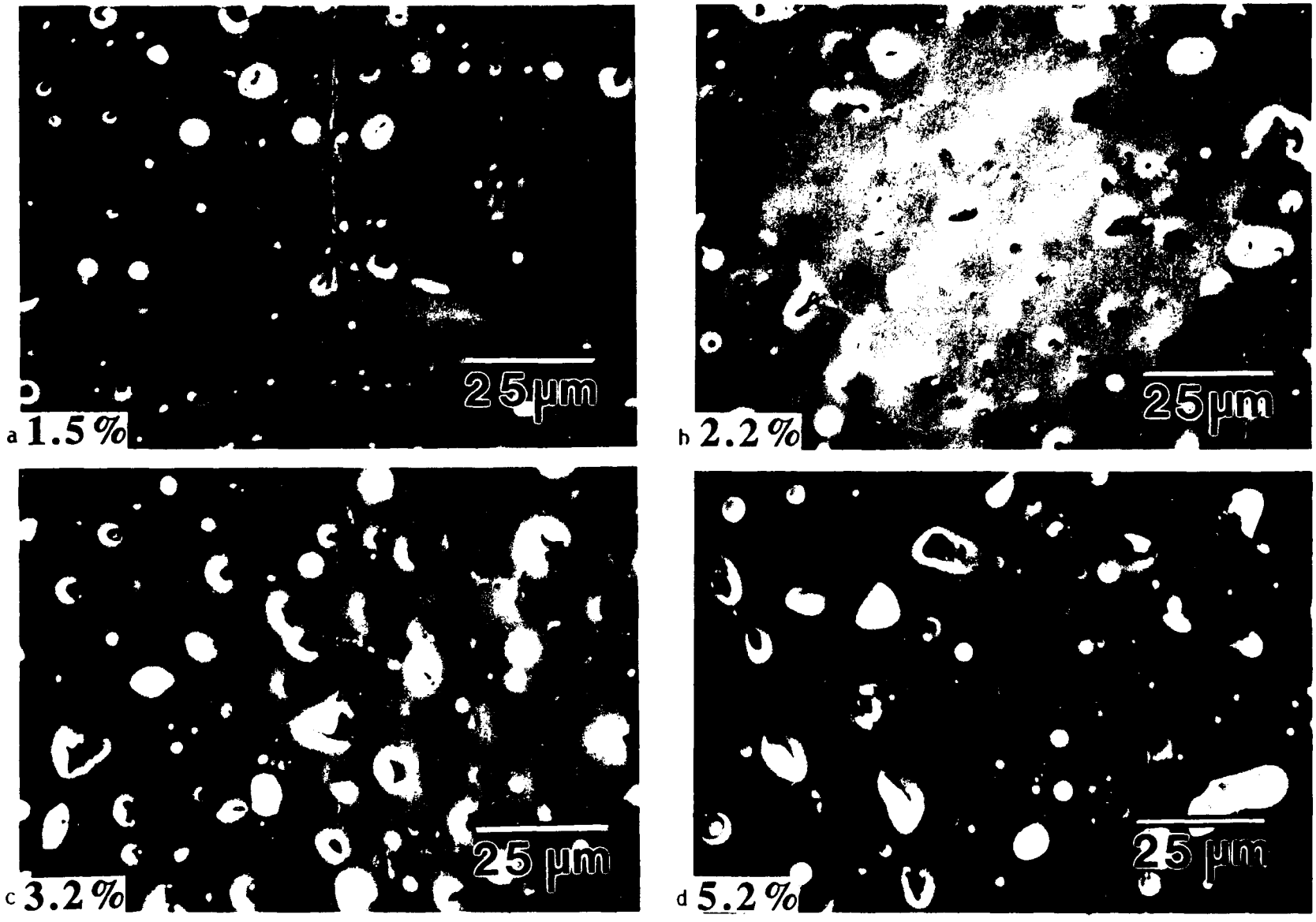

Fig. 2. Microstructures of 6061-T6 aluminum with 1.4 – 5.2 volume percent indium.

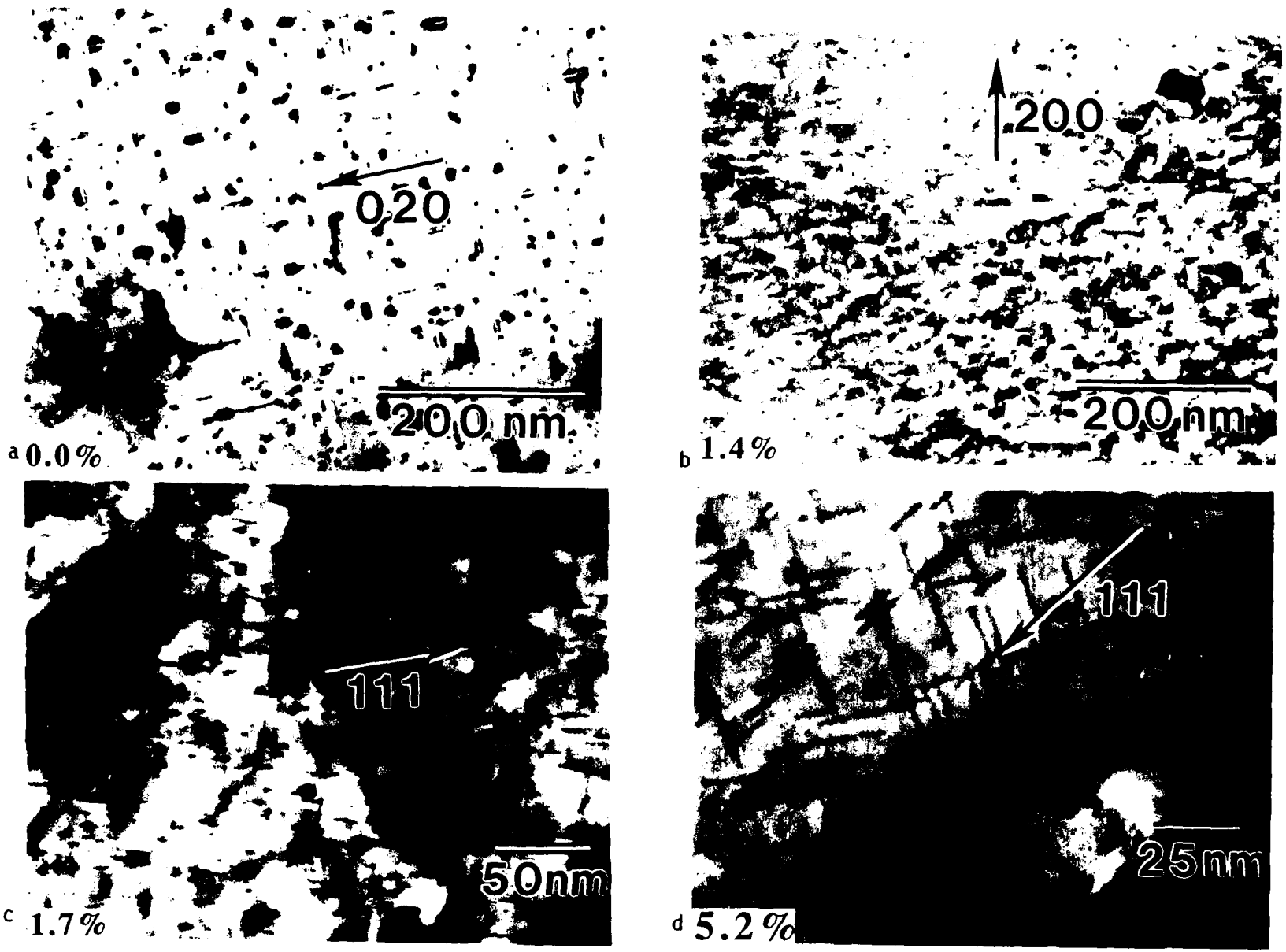

Fig 3. Precipitates in 6061-T6 aluminum with 0 – 5.2 volume percent indium.

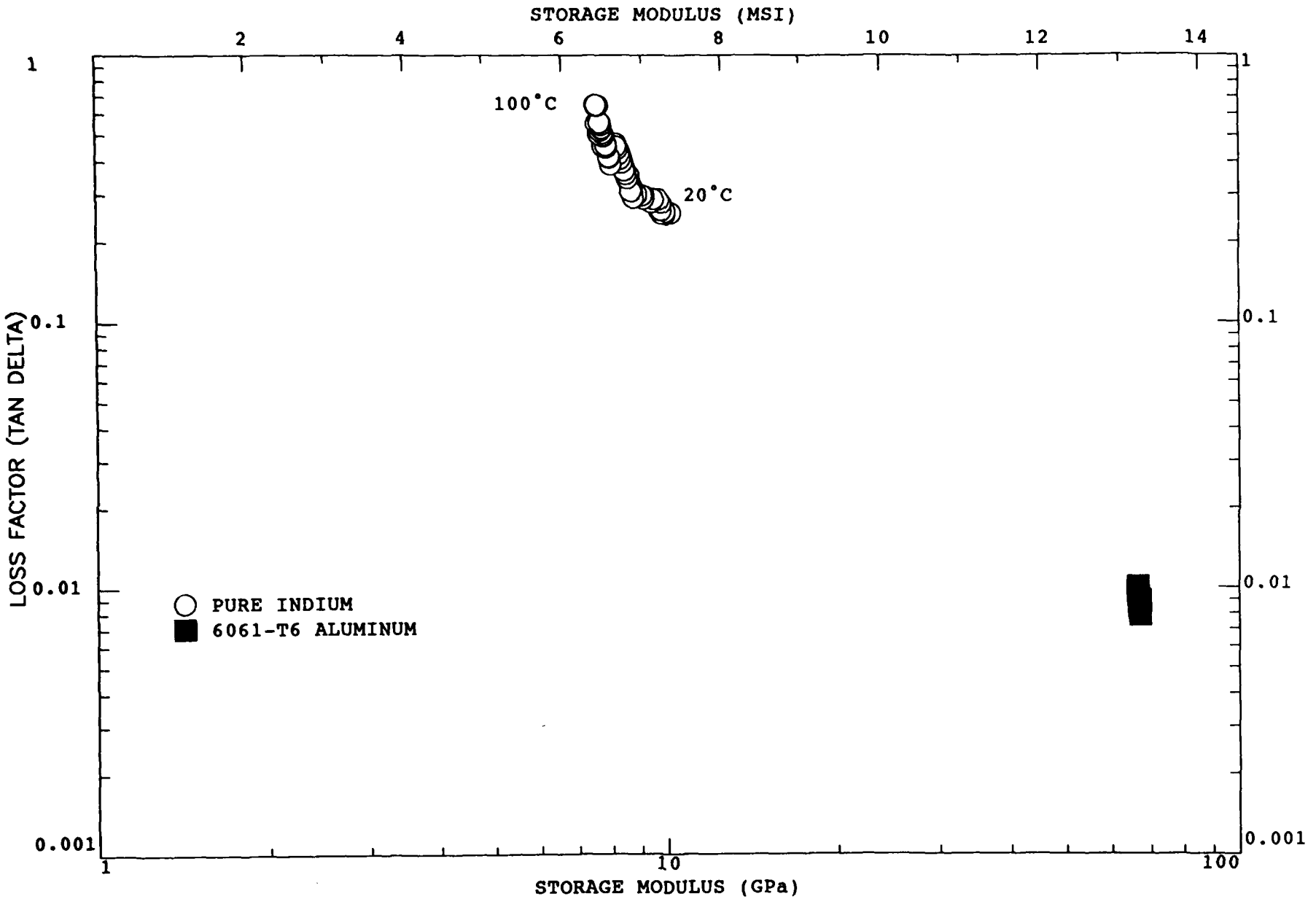

Fig. 4. Values of loss factor and storage modulus of the monolithic materials measured from 20 to 100°C at 0.1 Hz.

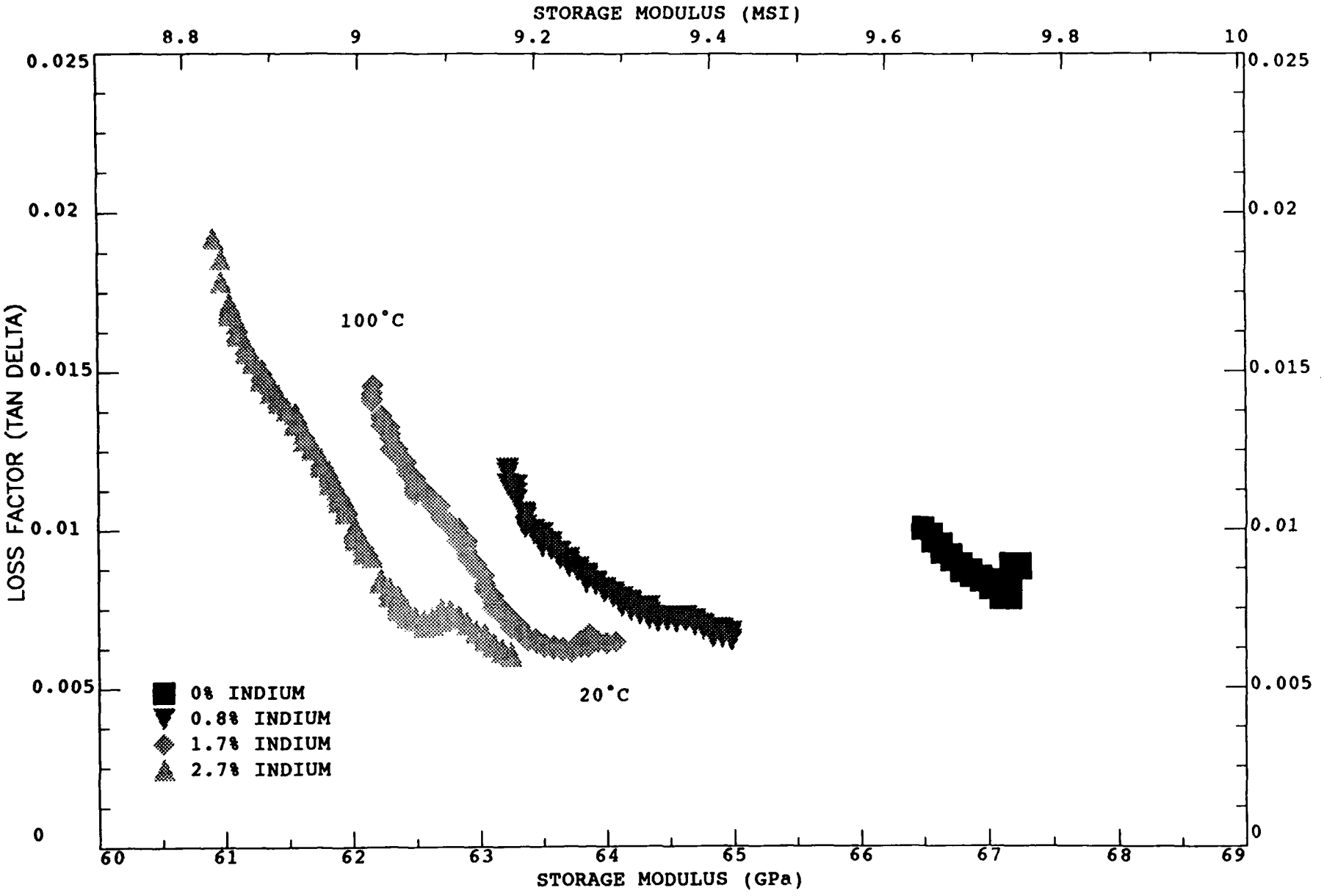

Fig. 5. Values of the loss factor and storage modulus of 6061 aluminum with 0 to 2.7 volume percent indium measured from 20 to 100°C at 0.1 Hz.

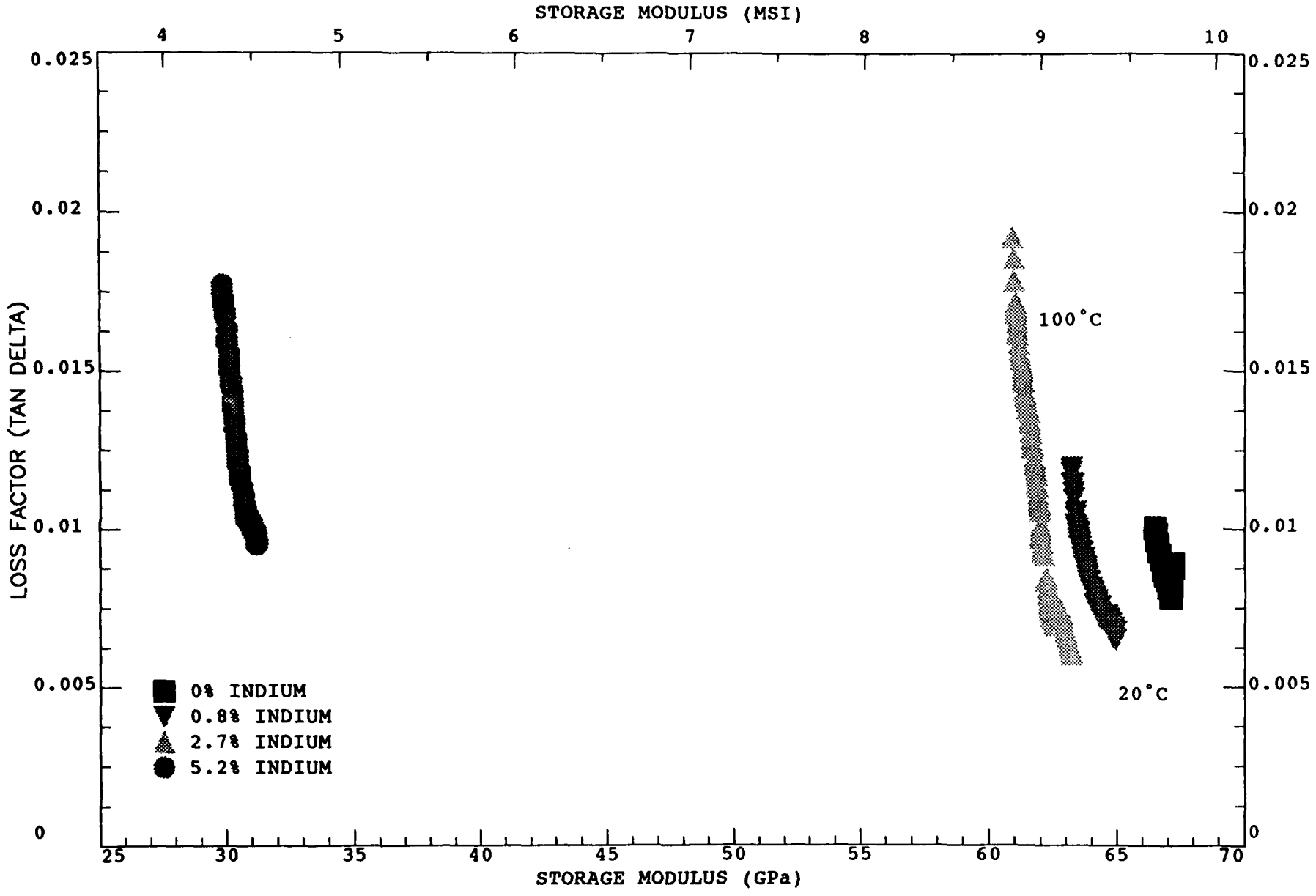

Fig. 6. Values of the loss factor and storage modulus of 6061 aluminum with 0 to 5.2 volume percent indium measured from 20 to 100°C at 0.1 Hz.

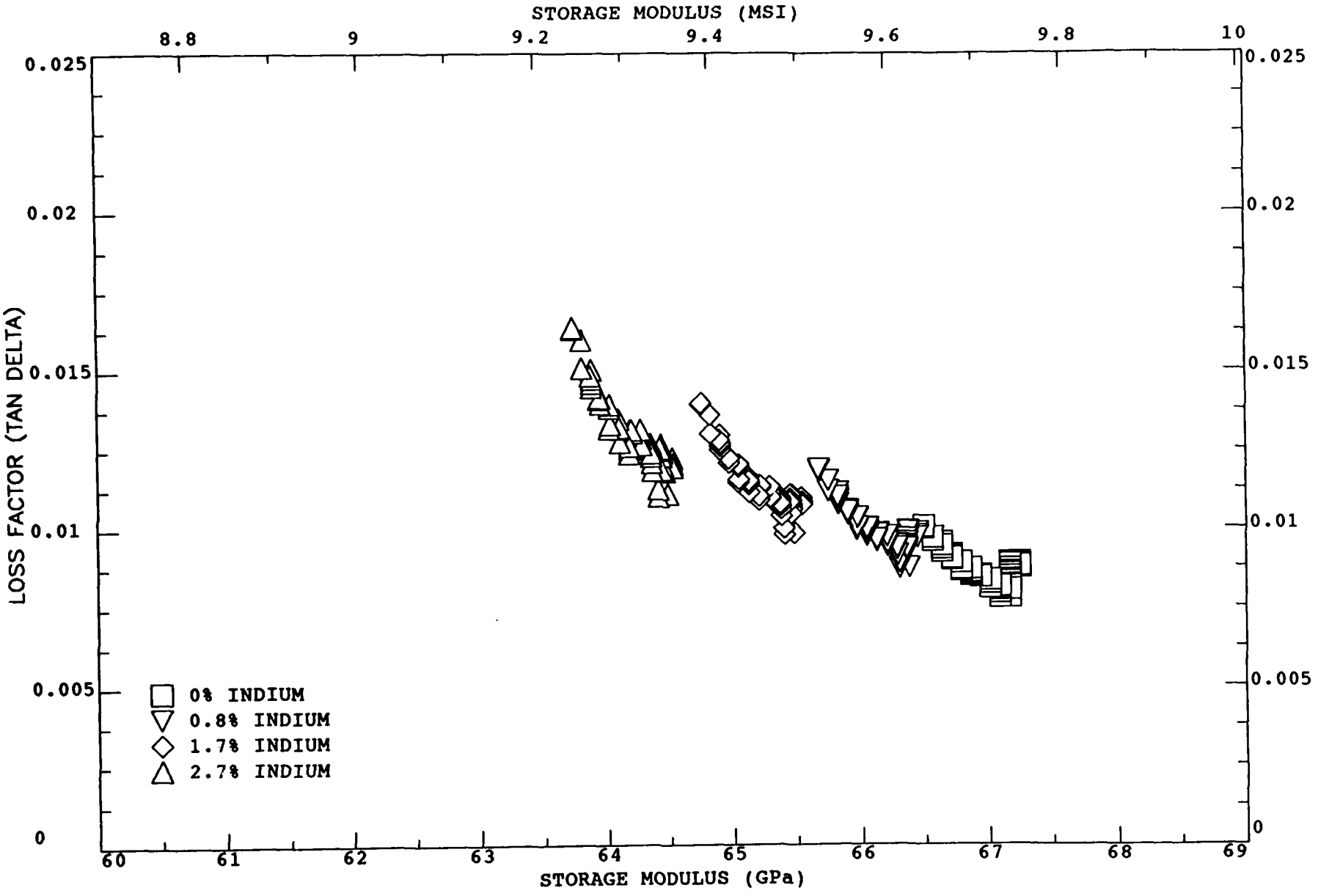

Fig. 7. Values of the loss factor and storage modulus of 6061 aluminum with 0 to 2.7 volume percent indium calculated using Nielsens model.

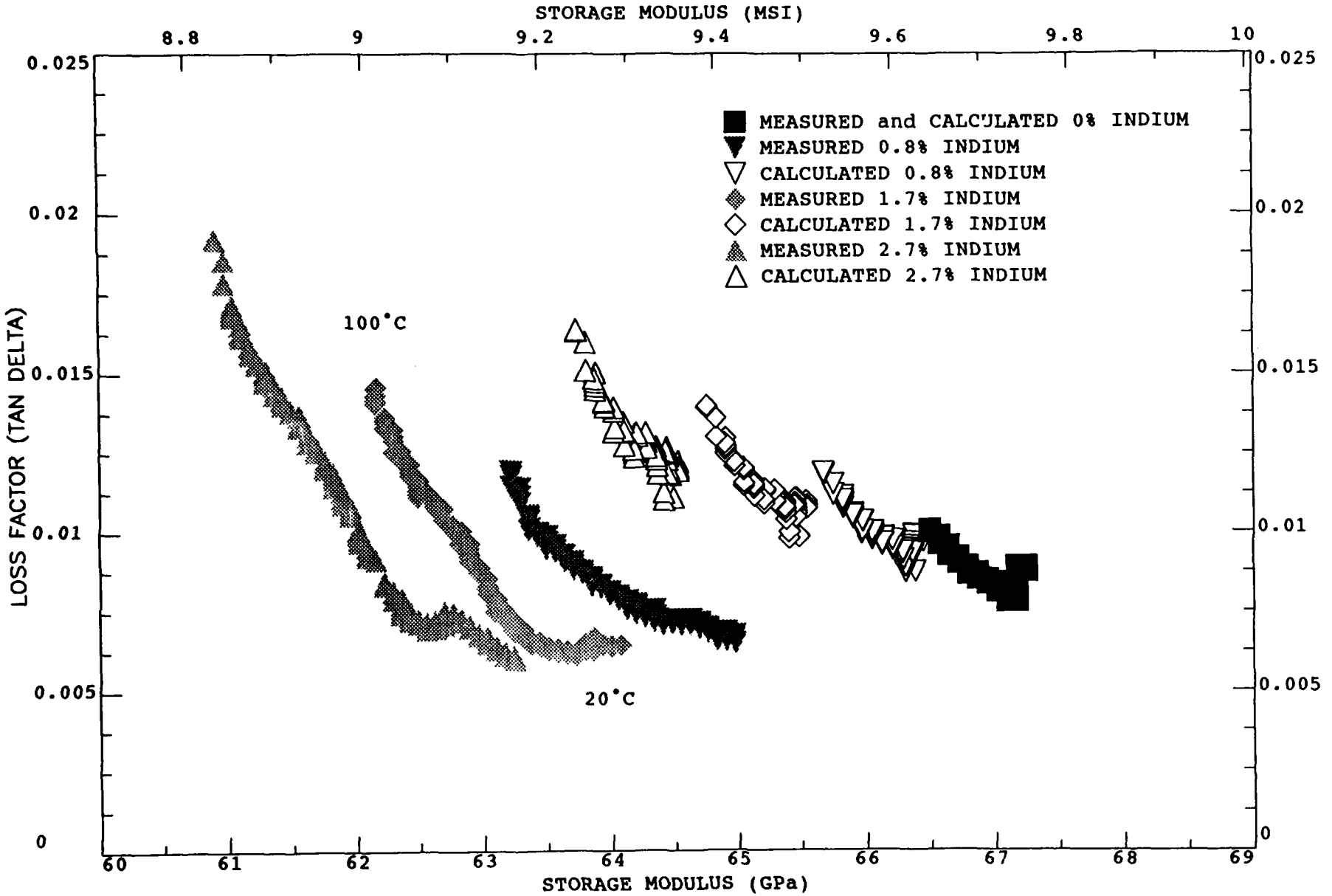

Fig. 8. Comparison of measured and calculated values of the loss factor and storage modulus of 6061 aluminum with 0 to 2.7 volume percent indium.

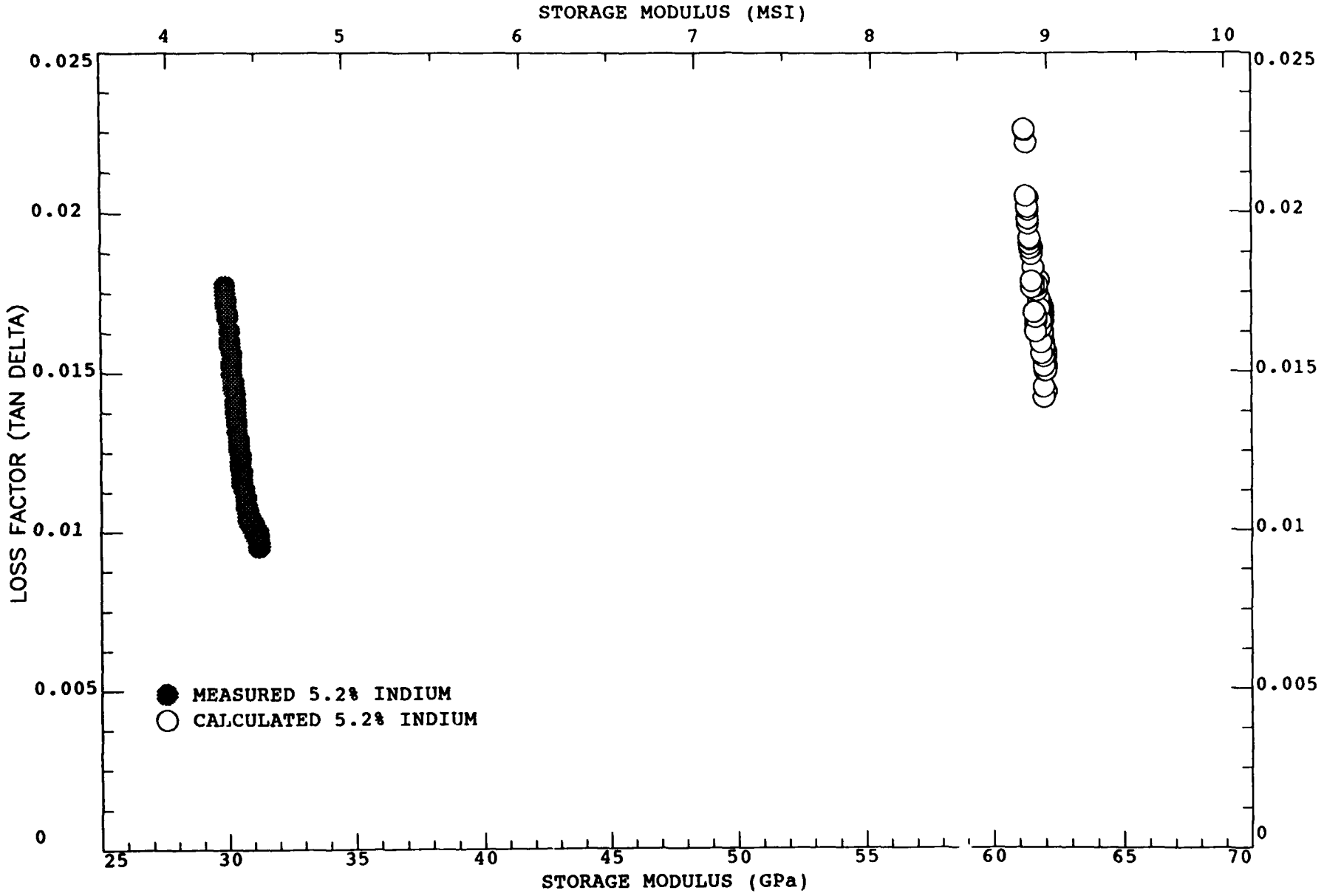

Fig. 9. Comparison of measured and calculated values of the loss factor and storage modulus of 6061 aluminum with 5.2 volume percent indium.

INITIAL DISTRIBUTION

Copies	
2	NRL
	Code 6323
	Code 6372
3	NAVPGSCOL
	Code 69PS
15	NAVSEA
	SEA 05M
	SEA 05MB
	SEA 05M2
	SEA 05M3
	SEA 05R25
	SEA 08
	SEA 55Y
	SEA 55Y1
	SEA 55Y12
	SEA 55Y2
	SEA 55Y21
	SEA 55Y22
	SEA 55Y3
	SEA 55Y31
	SEA 9612
12	DTIC
3	Dr. David Van Aken Dept. Materials Science and Engineering University of Michigan Ann Arbor, MI 48109

CENTER DISTRIBUTION

Copies	Code
1	0115
1	1905.1
1	1961
1	1962
1	1965 (RJD)
1	2742
1	2749
1	28 (Wacker)
1	2801 (Crisci)
1	2801 (Ventriglio)
1	2802 (Morton)
1	2803 (Cavallaro)
1	2803 (Hardy)
1	2809 (Malec)
5	281 (Gudas)
5	2812
10	2812 (C.Wong)
1	283 (Singerman)
1	284 (Fischer)
1	2844
1	522.1
1	522.2
2	5231